Title
Feasibility Study of a Partially Hollow Configuration for Zirconia Dental Implants

Journal
Journal of Oral and Maxillofacial Surgery, 68(2)

ISSN
0095-9618

Authors
Zhu, Jinwen
Yang, Dong-Wei
Ma, Fai

Publication Date
2010-02-01

DOI
10.1016/j.joms.2009.10.001

Peer reviewed

Feasibility Study of a Partially Hollow Configuration for Zirconia Dental Implants

Jinwen Zhu, PhD, Dong-Wei Yang, DDS,† and Fai Ma, PhD‡*

Purpose: To assess the feasibility of a new shape configuration involving a partially hollow and porous lower part for dental implants.

Materials and Methods: Cylindrical zirconia dental implants coated with bioactive glass were fabricated in the laboratory. Each implant has a solid upper part and a partially hollow lower part. It is open at the bottom with holes through the lower cylindrical walls. This hollow and porous configuration permits bone growth into the lower part of the implant that, over time, forms an interlinked network to lock the implant into the alveolar bone. Biomechanical properties of the new design were evaluated through material testing and experiments with dogs.

Results: Mechanical testing of bending strength, hardness, fracture toughness, and fatigue life indicated that zirconia implants with the proposed partially hollow configuration can be fabricated to have structural properties comparable to or exceeding the usual requirements for implants. Animal testing suggests that there is appreciable improvement in lock-in strength and osteointegration due to the hollow and porous configuration.

Conclusion: The new shape configuration is biomechanically feasible and further research is warranted to improve the design for human use.

J Oral Maxillofac Surg 68:399-406, 2010

In the past 3 decades, many different materials and shapes have been proposed for dental implants. In the area of materials, it is generally accepted that implants made of zirconia ceramics with bioactive glass coatings are superior. Zirconia is stable and nontoxic, and the bioactive coatings bond with the surrounding tissues to increase adhesion to bone structure.[1-5] In the area of implant shape the situation is less convergent. Many shapes have been used in implant design, each with its own merits and disadvantages. A basic requirement for the shape, whether smooth or threaded, is that the implant must withstand biting forces and safely transfer these forces to interfacial tissues. Siegele and Soltesz[6] found that the interfacial stress distribution of an implant with small protrusions or geometric discontinuities was much higher than that with a smooth exterior contour. Patra et al[7] and Mailth et al[8] compared the interfacial stress concentrations between cylindrical and conical implants and concluded that cylindrical implants were more dispersive in stress. Using titanium implants, Tsutsumi et al[9] found by finite-element analysis (FEM) that an optimal shape was cylindrical. A survey of the effect of implant shape on stress was recently provided by Szucs et al[10,11] and Lee et al.[12]

In this report, a new shape configuration is proposed to improve the long-term lock-in strength of zirconia dental implants inside the alveolar bone. The new implant shape involves a solid upper part and a hollow lower part. It is open at the bottom with holes through the lower walls. Compared with a solid implant, this hollow and porous shape configuration permits bone growth into the lower part of the implant after prosthodontics that, over time, can lock the implant into the alveolar bone and thus improve

*Postdoctoral Fellow, Department of Materials Science and Engineering, Tsinghua University, Beijing, China.

†Deputy Chief, Oral Surgery, Mei Tan General Hospital, Beijing, China.

‡Professor of Applied Mechanics, Department of Mechanical Engineering, University of California, Berkeley, CA.

Address correspondence and reprint requests to Dr Zhu: Advanced Materials Laboratory, Department of Materials Science and Engineering, Tsinghua University, Beijing 100084, China; e-mail: jinwenzhu2004@yahoo.com.cn

0278-2391/10/6802-0026$36.00/0
doi:10.1016/j.joms.2009.10.001

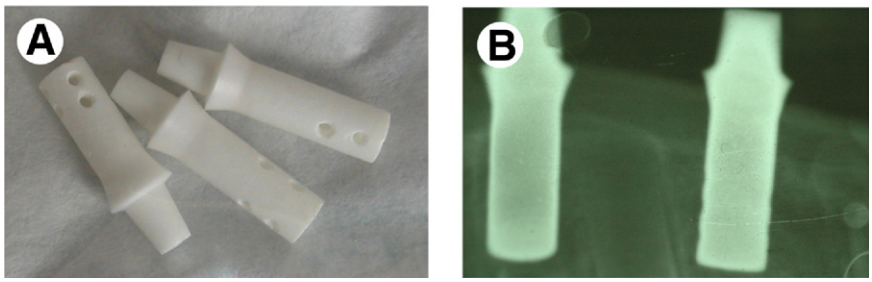

FIGURE 1. *A,* Partially hollow zirconia implants coated with bioactive glass. *B,* X-ray photograph of zirconia implants in the mandible of a dog.

Zhu, Yang, and Ma. Zirconia Dental Implants. J Oral Maxillofac Surg 2010.

rigidity. To evaluate the feasibility of the new configuration, implants with a cylindrical exterior and a cylindrical interior cavity were used. Although a smooth cylindrical exterior was chosen for this feasibility study, it would certainly be possible to use a threaded cylindrical shape or even a different exterior shape.

Sample implants, shown in Figure 1, were fabricated in the laboratory with high-density zirconia substrates and coated with bioactive glass and induced enzyme. The exterior and interior contours of the cylindrical implant were evaluated by FEM and somewhat optimized. For example, the neck near the top of the implant was shaped to reduce stress concentrations at the jawbone level. To determine whether such a partially hollow and porous configuration is biomechanically feasible, mechanical and animal tests were conducted. A fundamental objective of this report is to describe the findings of this feasibility study. Although a limited set of data is presented, more extensive testing has been performed by the authors to support any qualitative results given herein.

Materials and Methods

FABRICATION AND DIMENSIONS OF IMPLANTS

Each sample implant shown in Figure 1 has a length of 18.4 mm and a diameter of 4.1 mm below the neck. It is made of zirconia ceramics and coated with bioactive glass and induced enzyme. When partially stabilized by yttrium, zirconia ceramics (YPSZ) can reach a very high level of osteointegration. Two different types of YPSZ substrates were used for the fabrication of implants in the laboratory. The compositions of #1 and #2 substrates are listed in Table 1. The zirconia implants were prepared by extrusion from a paste consisting of organic additives and 90% weight of pure, medical-grade YPSZ powders. After drying, the extruded samples were fired in a laboratory kiln to final temperatures of 1,400°C for #1 substrate and 1,600°C for #2 substrate, at a heating rate of 100°C/hour. The substrates were kept at their respective maximum temperature for 1 hour and then cooled down to room temperature at a rate of 200°C/hour. All sintered samples were accurately sized and rectified. Afterward, an interior central cylindrical cavity of 5.5 mm in length and 2 mm in diameter was made in the lower part of each cylindrical implant by laser processing. In addition, circular holes of 0.5 mm in diameter were made in the lower cylindrical walls. The interior central cavity was open at the bottom and the circular holes were radial tunnels perpendicular to the longitudinal axis of the cylindrical implant. A cross-sectional view of the implant is depicted in Figure 2A. In contrast to the solid configuration shown in Figure 2C, the partially hollow and porous configuration permits fluid flow into the interior of the implant through the bottom opening and the tunnels.

Bioactive glass was applied as enamel to the surface of the YPSZ implants by brushing with a suitable slurry (with grain size <50 μm). After drying, all substrates were fired in a laboratory kiln at 1,280°C under vacuum. This process ensured good retention of the glass coatings on the surfaces of the YPSZ implants.[13] Ultimate tensile adhesion strength tests and profilometry analysis provided a coating bond strength of 32 ± 2 MPa, which indicated a good bond.[14]

TESTING OF MECHANICAL PROPERTIES

To evaluate the structural properties of the fabricated implants and to compare #1 with #2 implant substrates, several mechanical tests were conducted

Table 1. COMPOSITIONS OF 2 DIFFERENT ZIRCONIA SUBSTRATES

Substrate	Y_2O_3 (%wt)	Fe_2O_3 (%wt)	Na_2O (%wt)
#1	5.21 ± 0.20	≤ 0.01	≤ 0.04
#2	5.15 ± 0.20	≤ 0.01	≤ 0.04

Zhu, Yang, and Ma. Zirconia Dental Implants. J Oral Maxillofac Surg 2010.

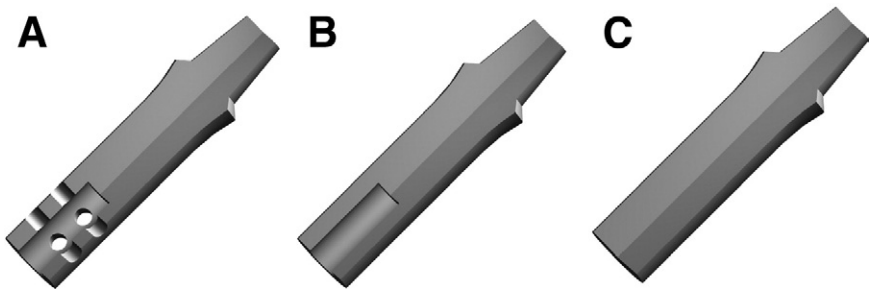

FIGURE 2. Cross-sectional views of 3 alternative designs for zirconia implants. *A*, Proposed hollow and porous configuration. *B*, Hollow but without radial tunnels. *C*, Solid configuration.

Zhu, Yang, and Ma. Zirconia Dental Implants. J Oral Maxillofac Surg 2010.

on uncoated implant specimens (without the bioactive glass coatings). These tests included bending strength, hardness, fracture toughness, and fatigue life of #1 and #2 substrates (Table 1). Bending strength refers to the resistance of a material to flexural deformations. It was assessed by measuring the failure stress in bending-mode tests (SJ-IA triaxial apparatus) to determine the limiting flexural strength σ_f.[15,16] Hardness refers to the resistance of a material to penetration by a pointed tool, and fracture toughness is defined as the resistance to brittle fracture in the presence of a crack. A diamond Vickers indentation machine with resolutions of ± 0.1 N for load measurements and ± 0.1 mm for depth measurements was used to generate the Vickers hardness numbers HV and fracture toughness factors K_{Ic}.[16] Fatigue refers to failure under a cyclic or alternating stress of amplitude that would not cause failure if applied only once. The slow fatigue crack propagation exponential, which characterizes fatigue life, was estimated from bending-mode experiments for #1 and #2 implant substrates.

IN VIVO STUDIES

To investigate the implant behavior in bone, 4 healthy adult female dogs were used in animal testing. The dogs were housed under standard conditions and supplied with food and water ad libitum. Each dog then received 4 #1 implants in the mandible. After 4 weeks, 2 dogs were euthanized and, after another 4 weeks, the remaining 2 were also euthanized. In each case the mandibles of the dogs were explanted and cleaned of soft tissues for morphologic investigations.

Sixteen implants were retrieved for in vivo studies. The retrieved implants and surrounding tissues were fixed in 4% paraformaldehyde for 7 days for undecalcified bone processing. Samples were dehydrated in a graded series of alcohols with increasing concentrations until a final grade of 100% was reached. They were then embedded in methylmethacrylate and sliced along a plane perpendicular to the longitudinal axis of the cylindrical implants. A series of sections of about 100 ± 20 μm thick, spaced 200 μm apart, were obtained with a Leica 1600 diamond saw microtome (Leica Microsystems, Nubloch, Germany). They were thinned to about 30 ± 5 μm by an exact polisher. The thinned sections were then coated with graphite to reduce static charges and viewed with a Zeiss MC80DX scanning electron microscope (SEM; Carl Zeiss Micro Imaging, Jena, Germany). This procedure allowed microstructures on the surfaces of the samples to be analyzed.

IMAGING OF MICROSCOPIC SURFACE PATTERNS

A Zeiss MC80DX SEM microscope was used to capture optical images of the zirconia implants at different stages of the experiments with various magnifications. In addition, an energy-dispersive spectrometer was used to evaluate the chemical composition of tissues on the surfaces of the implant coatings. The energy-dispersive spectrometer system is currently the commonest x-ray measurement system found in SEM laboratories. It offers a means of rapidly evaluating the constituents of a sample qualitatively and quantitatively.[17]

Results and Discussion

MECHANICAL TESTS

Bending strength, hardness, fracture toughness, and fatigue life of the 2 implant substrates were assessed and the results are presented in Table 2. It can be seen that #1 and #2 substrates possess structural properties comparable to or exceeding those of high-strength ceramics used in dental implants. However, the #1 implant substrate has greater bending strength and hardness than the #2 substrate, whereas the #2 implant substrate has greater fracture toughness and longer fatigue life. Perhaps this can be explained by the fact that the grain size of the #2 substrate is larger than that of the #1 substrate, which results in a reduction in strength and hardness but an increase in the capability of energy absorption and thus greater

Table 2. STRENGTH, HARDNESS, TOUGHNESS, AND FATIGUE OF #1 AND #2 ZIRCONIA SUBSTRATES

Substrate	Bending Strength σ_f (MPa)	Victors Hardness *HV* (GPa)	Fracture Toughness K_{Ic} (MPa)	SFCPE
#1	1035.43	12.99	4.27	13.41
#2	645.04	11.49	6.69	14.43

Abbreviation: SFCPE, slow fatigue crack propagation exponential.

Zhu, Yang, and Ma. Zirconia Dental Implants. J Oral Maxillofac Surg 2010.

fracture toughness and longer fatigue life. The #1 and #2 implants were used in animal tests.

To appreciate the relation between material grain size and hardness, specimens of #1 and #2 implant substrates were given pyramidal indentations with a square base using a diamond Vickers indentation machine with a compression force of 98 N. Optical images of the surfaces of the specimens were captured at ×200 magnification and are shown in Figure 3. It can be seen that the #1 substrate has finer grains, and its major crack extension emanating from the corners of the square has an approximate length of 273 μm. In contrast, the #2 substrate has larger grains, and a major crack extension of 189.8 μm approximately. The smaller grain size of the #1 substrate means greater material strength and hardness. Conversely, longer fault traces on the #1 substrate indicate that it is less capable of absorbing energy, resulting in a smaller value of fracture toughness and fatigue life.

STRESS DISTRIBUTIONS

As explained earlier, the new implant shape has a central cylindrical cavity of 5.5-mm length and 2-mm diameter open at the bottom. In addition, there are radial tunnels (circular holes) of 0.5-mm diameter perpendicular to the longitudinal axis of the cylindrical implant. The dimensions of the interior cavity and holes were chosen on an ad hoc basis to facilitate fabrication in the laboratory and, at the same time, to generate a reasonably large hollow space. Depending on the optimization criteria and constraints, these dimensions would likely change. Even on an ad hoc basis, many questions could be brought up. Would a change in the interior dimensions improve the interfacial stress distribution of the implant? Because an increase in the dimensions of the interior cylindrical space and radial tunnels could compromise the structural integrity of implant, it is not considered in this report. A decrease in the dimensions of the interior space would certainly not reduce the strength of the implant. By FEM, it was found that a reduction in the length and diameter of the interior cylindrical cavity did not change in any appreciable manner the stress distribution at the jawbone level. The same could be said about a decrease in the diameter and number of radial tunnels. Thus, stress distribution is rather insensitive to changes in interior dimensions. To the extent that structural integrity is not compromised, a large interior volume is generally preferred. A large interior cavity and radial tunnels will permit bone issues to grow easily into the implant and to form a strong network through the tunnels to increase implant rigidity.

As an illustration of the influence of interior dimensions on stress distributions, the 3 alternative designs shown in Figure 2 were analyzed (Fig 4). All 3 designs have the same exterior shape (18.4-mm length × 4.1-mm diameter). The proposed hollow and porous configuration is displayed in Figure 2A and the same design but without the radial tunnels is shown in Figure 2B. In contrast, a solid configuration is shown

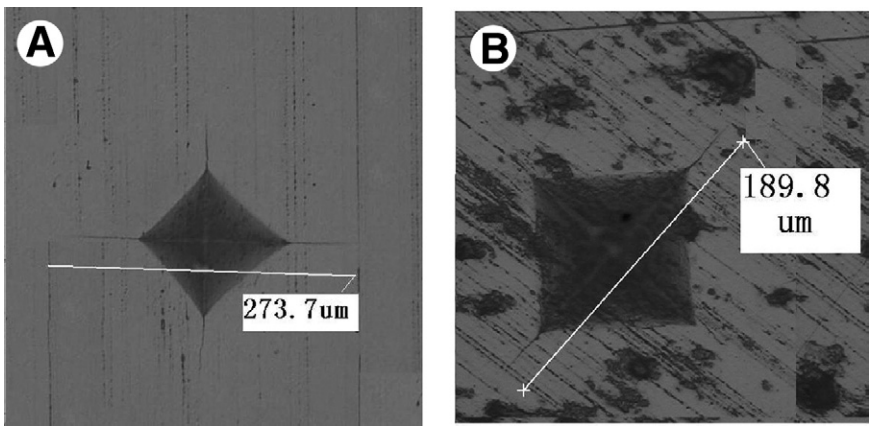

FIGURE 3. Optical images of pyramidal indentations and fault traces on surfaces of implant substrates at ×200 magnification. *A*, #1 Substrate. *B*, #2 Substrate.

Zhu, Yang, and Ma. Zirconia Dental Implants. J Oral Maxillofac Surg 2010.

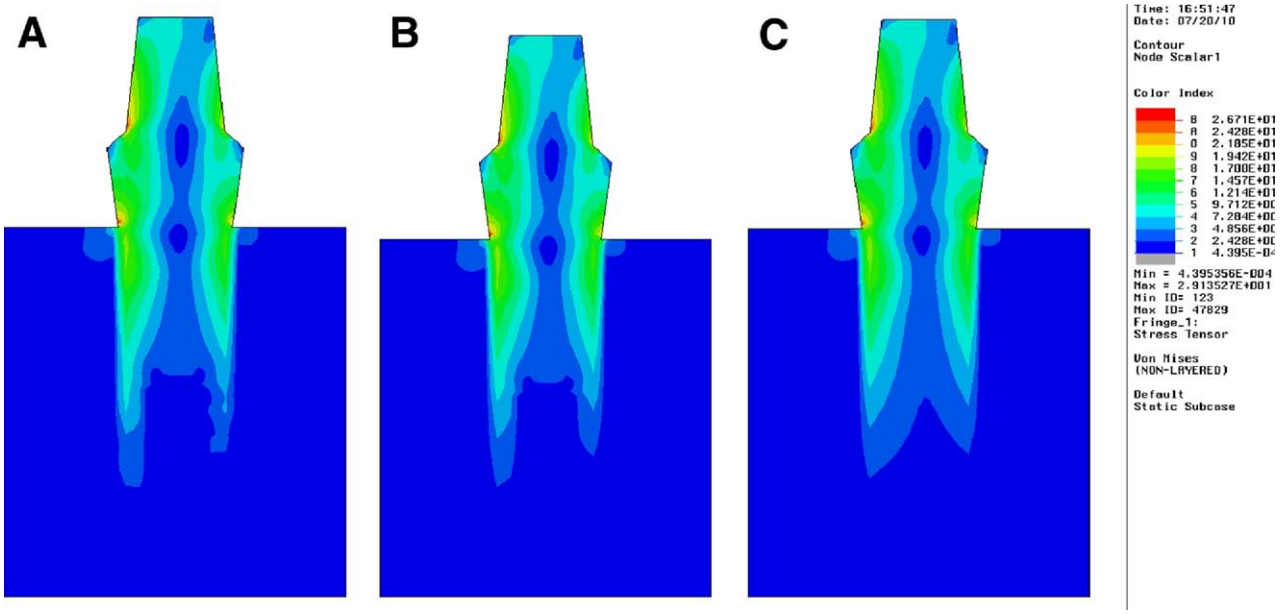

FIGURE 4. Stress distributions of the 3 alternative designs of Figure 2. *A*, Proposed hollow and porous configuration. *B*, Hollow but without radial tunnels. *C*, Solid configuration.

Zhu, Yang, and Ma. Zirconia Dental Implants. J Oral Maxillofac Surg 2010.

in Figure 2C. In FEM, an upward pressure of 2.4 MPa is applied to the 3 implants along the longitudinal direction.[18,19] At the same time a lateral concentrated force of 20 N perpendicular to the longitudinal axis is applied to the top of the implants. Assume that there is no relative motion between the implant and surrounding bone structure and that the implant has an embedded length of 11 mm inside the bone tissues. A 3-region FEM model was used to compute the stress distributions of the 3 designs shown in Figure 2. The 3 regions consisted of the implant, an upper layer of compact bone, and a lower area of cancellous bone. Material properties of the 3 regions are presented in Table 3. The resulting stress distributions of the 3 designs were computed and are shown in Figure 3. It is observed that the stress distributions are very similar near the jawbone level. Thus, modifications of the interior space near the bottom of the implant have little effect on the stress distributions at the jawbone level.

Table 3. MATERIAL PROPERTIES OF THE 3 REGIONS IN FINITE-ELEMENT ANALYSIS COMPUTATION OF STRESS DISTRIBUTIONS OF THE 3 ALTERNATE DESIGNS IN FIGURE 2

Material	Elastic Modulus (MPa)	Poisson Ratio (υ)
Zirconia	210,000	0.19
Compact bone	13,700	0.3
Cancellous bone	1,370	0.3

Zhu, Yang, and Ma. Zirconia Dental Implants. J Oral Maxillofac Surg 2010.

IN VIVO INVESTIGATIONS

In animal testing, there were no general or local complications with the 4 dogs after the placement of implants. The dogs remained in good health until they were euthanized. Micrographs of cross-sections of the retrieved implants and surrounding tissues are shown in Figure 5, in which the interior cavity and 1 radial tunnel are highlighted. These micrographs, obtained by backscattered electron imaging, demonstrate clearly that there was bone growth into the central interior cavity and radial tunnels. In addition, there was partial absorption with intergranular penetration of the bioactive glass coatings into the zirconia substrate. With SEM, it was estimated that the remaining coating thickness of bioactive glass alone was about 65 ± 12 μm 8 weeks after implantation. In comparison, the thickness of the layer of new bone tissues adjacent to the glass coatings was about 300 μm to 2 mm, which was relatively large. Certainly, the zirconia ceramics and bioactive glass coatings might account for the impressive bone infusion.[20] However, it is the interior cavity and radial tunnels that increase the contact area and permit bone growth into the lower part of the implant. Over time, bone growth inside and outside the implant results in an interlinked network that locks the implant into the alveolar bone to increase implant rigidity.

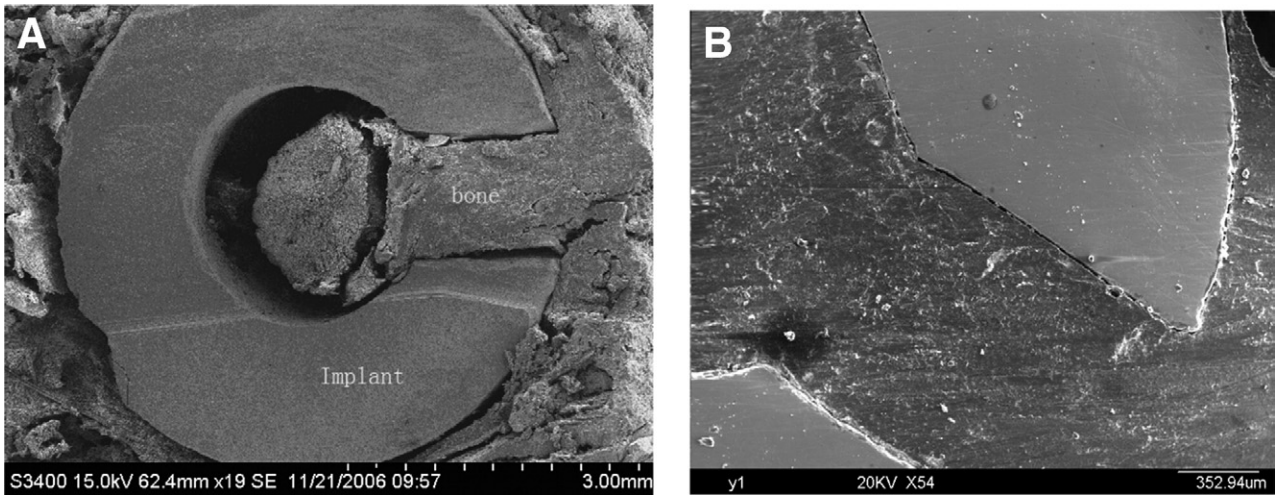

FIGURE 5. Cross-sections of zirconia implants showing newly formed bone tissues. *A*, Four weeks after implantation. *B*, Eight weeks after implantation.

Zhu, Yang, and Ma. Zirconia Dental Implants. J Oral Maxillofac Surg 2010.

A large number of micrographs were examined, and none contained any black spots to suggest inflammation around the implants.[21] All thinned samples examined by SEM revealed very good contact at the implant–bone interface. Tissue observations also indicated no abnormal inflammation. Thus, there was good osteointegration. Images of the implant surface, obtained by backscattered electron imaging, are shown in Figure 6. New bone growth on the surface could be seen 4 or 8 weeks after implantation, and an anomalous hydroxyapatite layer is visible in Figure 6B. The interface between implant and bone is shown in Figure 7, in which the bioactive glass coatings are represented by a vertical light-colored region in the middle of the figure. Although new bone grew on the glass coatings, the bioactive glass itself had partially diffused into the zirconia substrate. This was confirmed by the detection of bioactive glass components (silicon and calcium in particular) by energy-dispersive spectrometer, as shown in Figure 8. Measuring along a horizontal line in the middle of Figure 7, it was found that the thickness of bioactive glass layer diminished by about 40 μm 4 to 8 weeks after implantation. This adsorption of bioactive glass was greater than previously reported.[22-24] In the past implant ceramics were molded with die-pressing, whereas the implants fabricated in this feasibility study were made by extrusion, which produced slightly less dense ceramics. Perhaps this made it easier for the glass to be absorbed into zirconia substrate. Overall, it was the adsorption of the glass coatings into zirconia and the growth of bone on the glass coatings, inside and outside the zirconia implant, that contributed to improved implant rigidity. For implants made of less biocompat-

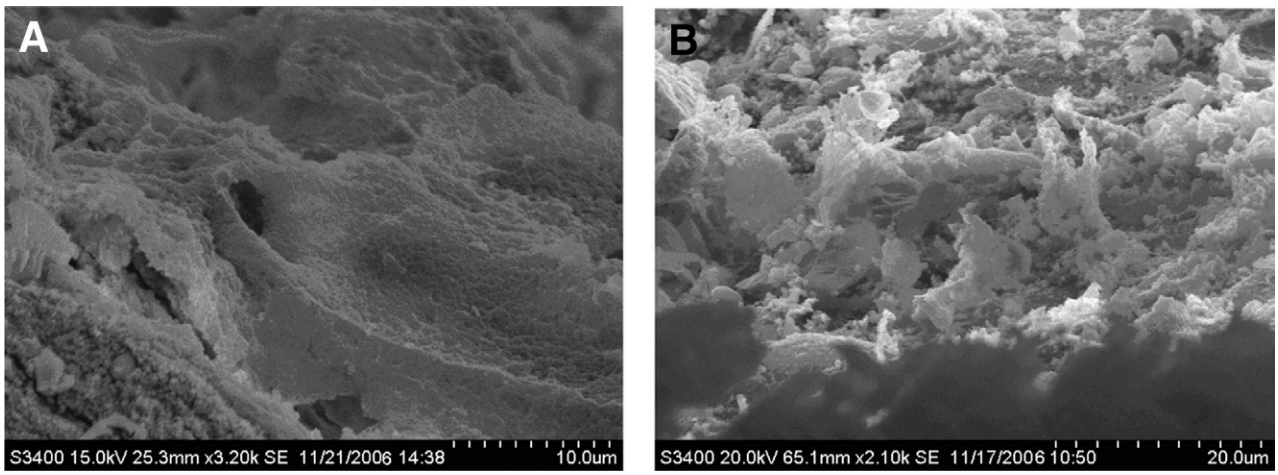

FIGURE 6. SEM morphologies of implant surface. *A*, Four weeks after implantation. *B*, Eight weeks after implantation.

Zhu, Yang, and Ma. Zirconia Dental Implants. J Oral Maxillofac Surg 2010.

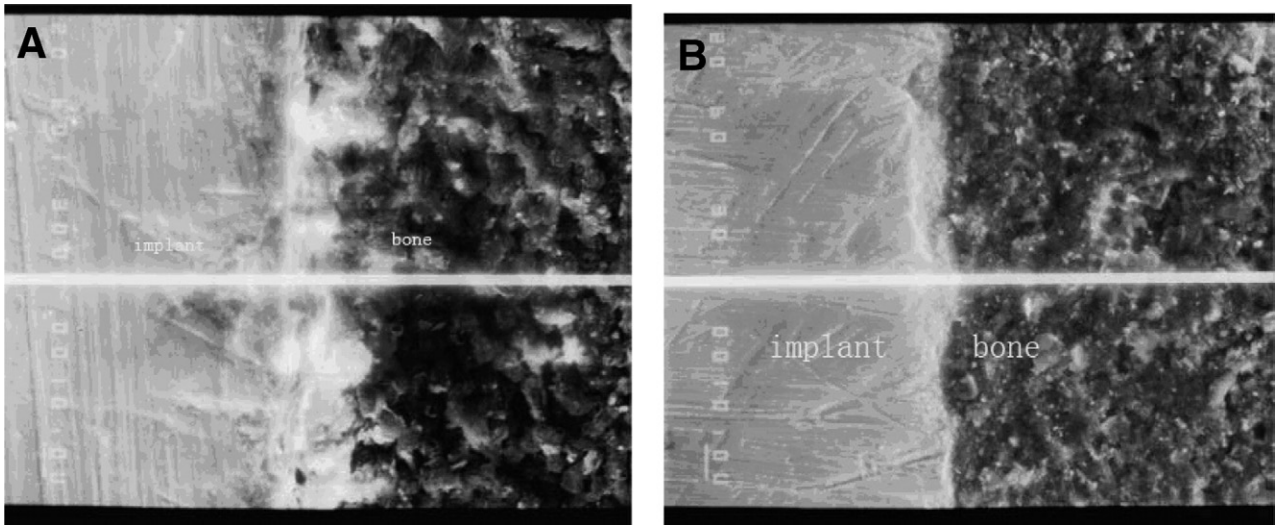

FIGURE 7. SEM morphologies of the interface between implant and live bone. *A*, Four weeks after implantation. *B*, Eight weeks after implantation.

Zhu, Yang, and Ma. Zirconia Dental Implants. J Oral Maxillofac Surg 2010.

ible materials and without any bioactive coatings, bone growth into the implant might require a longer period but the hollow and porous configuration would still impart greater implant rigidity.

In conclusion, the feasibility of a new shape configuration for dental implants has been assessed in this report. The new implant configuration involves a solid upper part and a hollow lower part that is open at the bottom with radial tunnels (circular holes) through the lower walls. The implants used in this feasibility study were made of zirconia ceramics and coated with bioactive glass. This partially hollow and porous configuration permits bone growth into the lower part of the implant that, over time, locks the implant into the alveolar bone. Biomechanical properties of the new design have been evaluated through material testing and experiments with dogs.

Based on an evaluation of bending strength, hardness, fracture toughness, and fatigue life of implant substrates, it has been shown that implants with the new shape configuration can be fabricated to have structural properties comparable to or exceeding the usual requirements for implants. In addition, the stress distribution of the implant at the jawbone level is rather insensitive to changes in the dimensions of the interior cavity and to the size and number of radial tun-

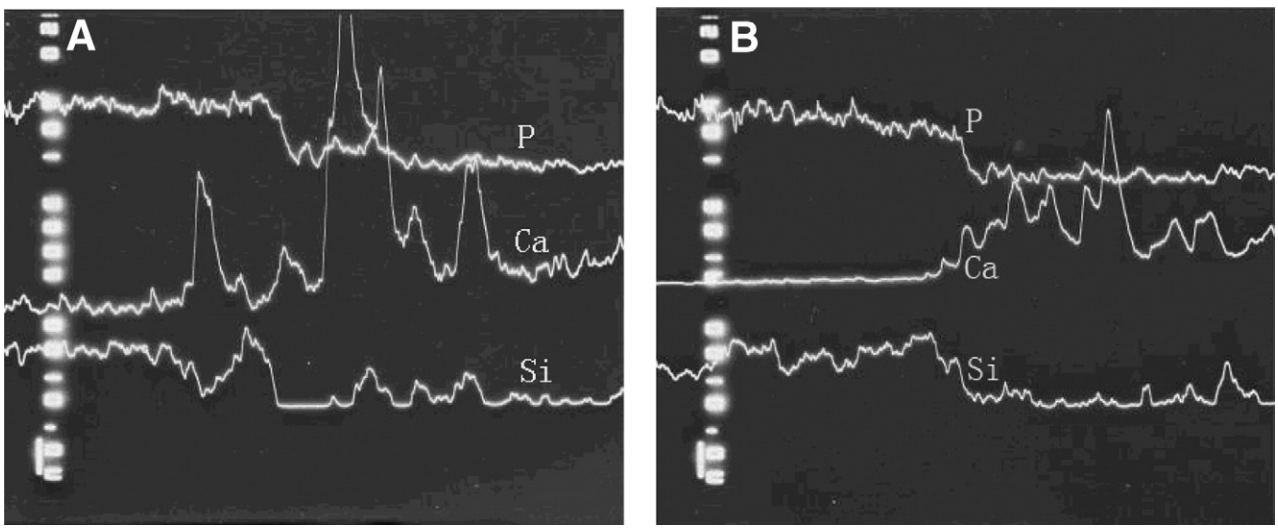

FIGURE 8. Energy-dispersive spectrometric line scan of the interface between implant and live bone. *A*, Four weeks after implantation. *B*, Eight weeks after implantation.

Zhu, Yang, and Ma. Zirconia Dental Implants. J Oral Maxillofac Surg 2010.

nels. In animal testing with dogs, it has been observed that there is appreciable bone growth into the interior cavity and radial tunnels of the implants. This bone growth results in the formation of an interlinked network of tissues through the tunnels and the bottom opening to increase implant rigidity. Although a limited set of data is presented, extensive testing has been performed by the authors to support any qualitative statements given herein. Overall, it has been found that the new shape configuration is biomechanically feasible and further research is warranted to improve the design for human use.

References

1. Att W, Kurun S, Gerds T, et al: Fracture resistance of single-tooth implant-supported all-ceramic restorations: An in vitro study. J Prosthet Dent 95:111, 2006
2. Schulze MS, Schliephake H, Radespiel TM, et al: Osteointegration of endodontic endosseous cones: Zirconium oxide vs titanium. Oral Surg Oral Med Oral Pathol Oral Radiol Endod 89:91, 2000
3. Willmann G: Standardization of zirconia ceramics for hip endoprostheses. Biomed Tech (Berl) 42:342, 1997
4. Shimizu K, Oka M, Kumar P, Kotoura Y, et al: Time dependent changes in the mechanical properties of zirconia ceramic. J Biomed Mater Res 27:729, 1993
5. Fini M, Giavariesi G, Torricelli P, et al: Biocompatibility and osteointegration in osteoporotic bone. J Bone Joint Surg Br 83:139, 2001
6. Siegele DS, Soltesz U: Numerical investigations of the influence of implant shape on stress distribution in the jaw bone. Int J Oral Maxillofac Implants 4:40, 1989
7. Patra AK, Depaolo JM, Souza KS, et al: Guidelines for analysis and redesign of dental implants. Implant Dent 7:68, 1998
8. Mailth G, Stoiber B, Watzek G, et al: Bone resorption at the entry of osseointegrated implants—A biomechanical phenomenon. Z Stomatol 86:207, 1989
9. Tsutsumi S, Fukuda Y, Tani Y: Biomechanical designing of implants. J Dent Res 68:754, 1989
10. Szucs A, Divinyi T, Lorincz A, et al: A biomechanical study of the mechanical stress transmission of dental implants using finite element analysis. Part I. Review of literature. Fogorv Sz 99:141, 2006
11. Szucs A, Divinyi T, Bojtár I: A biomechanical study of the mechanical stress transmission of dental implants using finite element analysis. Part II. Experiments. Fogorv Sz 99:187, 2006
12. Lee JH, Frias V, Lee KW, et al: Effect of implant size and shape on implant success rates: A literature review. J Prosthet Dent 94:377, 2005
13. Ferraris M, Verne E, Appendino P, et al: Coatings of zirconia for medical applications. Biomaterials 21:765, 2000
14. Krajewski A, Ravaglioli A, Mazzocchi M, et al: Coating of ZrO_2 supports with biological glass. J Mater Sci Mater Med 9:309, 1998
15. Hosford WF: Mechanical Behavior of Materials. New York, Cambridge University Press, 2005, p 53
16. Dowling NE: Mechanical Behavior of Materials (ed 3). Upper Saddle River, NJ, Prentice-Hall, 2007, p 101
17. Otulakowska J, Nicholson JW: Scanning electron microscopy and energy dispersive X-ray study of a recovered dental implant. Mater Sci Mater Med 17:277, 2006
18. Holmgren EP, Seckinger RJ, Kilgren LM, et al: Evaluating parameters of osseointegrated dental implants using finite element analysis—A two-dimensional comparative study examining the effects of implant diameter, implant shape and load direction. Oral Implantol 24:65, 1998
19. Hongyue L, Zhu L, Zedong L, et al: The effects of implant shapes on stress distribution in implant-bone interface. Chin J Oral Implantol 8:61, 2003
20. Greenspan, DC: Bioactive ceramic implant materials. Curr Opin Solid State Mat Sci 4:389, 1999
21. Stanic V, Aldini NN, Fini M, et al: Osteointegration of bioactive glass-coated zirconia in healthy bone: An in vivo evaluation. Biomaterials 23:3833, 2002
22. Kim HW, Georgiou G, Knowles JC, et al: Calcium phosphates and glass composite coatings on zirconia for enhanced biocompatibility. Biomaterials 25:4203, 2004
23. Neo M, Nakamura T, Ohtsuki C, et al: Apatite formation on three kinds of bioactive material at an early stage in vivo: A comparative study by transmission electron microscopy. J Biomed Mater Res 27:999, 1993
24. He Z, Ma J, Wang C: Constitutive modeling of the densification and the grain growth of hydroxyapatite ceramics. Biomaterials 26:1613, 2005